



The Society shall not be responsible for statements or opinions advanced in papers or discussion at meetings of the Society or of its Divisions or Sections, or printed in its publications. Discussion is printed only if the paper is published in an ASME Journal. Authorization to photocopy for internal or personal use is granted to libraries and other users registered with the Copyright Clearance Center (CCC) provided \$3/article or \$4/page is paid to CCC, 222 Rosewood Dr., Danvers, MA 01923. Requests for special permission or bulk reproduction should be addressed to the ASME Technical Publishing Department.

Copyright © 1998 by ASME

All Rights Reserved

Printed in U.S.A.

**APPLICATION OF STRESS RELAXATION TESTING IN METALLURGICAL LIFE
ASSESSMENT EVALUATIONS OF GTD111 ALLOY TURBINE BUCKETS**

Joseph A. Daleo BWD TURBINES LIMITED, Ancaster, Ontario, Canada
Keith A. Ellison BWD TURBINES LIMITED, Ancaster, Ontario, Canada
David A. Woodford MATERIALS PERFORMANCE analysis, Inc.
Santa Barbara, California, USA



ABSTRACT:

Stress relaxation and constant displacement rate tensile tests were performed on poly-crystalline GTD111 alloy material removed from General Electric MS6001B first stage combustion turbine buckets. Samples were examined in the standard heat treated condition, thermally exposed at 900°C for 5000 hours and from service run buckets. Creep rates of the material were measured and evaluated directly in terms of temperature capability at 850°C and 900°C. Stress relaxation tests done at 0.8% total strain indicated that the creep rate properties in the service exposed airfoil were an order of magnitude higher than the material properties in the standard heat treated condition measured in the root form. In terms of temperature capability, the creep rate properties of the service run airfoil material had decreased by the equivalent of almost 40°C.

The stress relaxation test method was demonstrated to be a very useful tool in quantifying the degradation of creep properties in service run components. Creep data that would require years to gather using conventional creep tests was generated in a few days. This now makes realistic life assessment and repair / replace decisions possible during turbine overhauls.

The test method's unique ability to measure changes in creep rate over a large stress range, enabled the technique to distinguish between changes in creep strength due to (normal) microstructural evolution from the combined effects of microstructural evolution and strain related creep damage.

A method for estimating standard constant load creep rupture life from the stress relaxation creep rate data is also presented along with time-temperature parameter correlations. The data sets examined in this study indicate that creep rupture lives can be estimated within a factor of three from the stress relaxation data.

The information and analysis techniques described in this paper are directly applicable to metallurgical life assessment evaluations and the re-qualification of repaired General Electric buckets in Frame 3, 5, 6, 7 and 9 engine models.

INTRODUCTION

The maintenance period of critical gas turbine components operating in advanced technology industrial turbines is often determined by the material's long term metallurgical stability at the actual operating conditions encountered in service. The progressively higher firing temperatures used in all of the advanced engine designs results not only in very high metal surface temperatures but also in very high temperature gradients and concomitant thermal stresses, induced in part by the complex cooling systems. Unexpected changes in alloy properties due to higher than expected operating temperatures or stress can result in poor structural performance of the component design and reduced life.

Operating conditions can dramatically affect the life of gas turbine hot section buckets. An understanding of the original design parameters and their affect on component life is essential to understanding degradation modes resulting from "off design" operation. Today's advanced alloy/coating systems are expected to withstand very high temperatures and stresses for periods up to 48,000 hours. Steady state centrifugal stresses range from a few MPa to 250 Mpa, however, the thermal stress in the airfoil due to temperature gradients can range from -350 MPa to 500Mpa. Typical steady state metal temperatures range from 760°C to 985°C. It is very clear from the temperature and stress estimates that the base alloy and coating systems degrade with time and as longer hours of service are accumulated, maintenance considerations such as developing optimum component life strategies and repair processes become important.

Presented at the International Gas Turbine & Aeroengine Congress & Exhibition
Stockholm, Sweden — June 2–June 5, 1998

This paper has been accepted for publication in the Transactions of the ASME
Discussion of It will be accepted at ASME Headquarters until September 30, 1998

Downloaded from http://asmedigitalcollection.asme.org/GT/proceedings-pdf/GT1998/78668/V005T12A001/4218593/v005t12a001-98-gt-370.pdf by guest on 03 December 2022

Metallurgical life assessment of service-exposed buckets has proven to be the most effective means of identifying the important modes of material degradation affecting component life. Methods for performing comprehensive metallurgical life assessments and failure analysis of gas turbine components have been recently described by Daleo and Boone (1996).

As part of the metallurgical analysis, the degradation of material properties is estimated, by performing mechanical tests on material taken from critical areas of representative components. The remaining creep strength is usually evaluated by conducting short-term, accelerated creep rupture tests at temperatures and/or stresses that are higher than those actually encountered in service. These tests were originally developed as standard quality control tests for new materials to quickly screen out chemistry lots and heat treatment cycles that produced properties outside of the normal scatter band.

One objection to the use of short term creep tests to predict long term behavior arises from the fact that microstructural changes that occur during service reduce the creep rupture lives of test specimens tested at low to intermediate temperatures at high stress levels, but have a much smaller effect on long term rupture lives at stresses and temperatures which are more typical of those actually encountered in service (Koul and Castillo, 1993). This can, and often does, lead to very conservative recommendations being made to replace or HIP reheat treat buckets prematurely.

EXPERIMENTAL PROGRAM

The experimental program was designed to determine if the stress relaxation test method would be able to distinguish between the various material conditions which could be present in service exposed gas turbine components:

1. Reduction in creep properties due primarily to environmental and microstructural changes (e.g. vane segments, solid first and second stage rotating blades or buckets operating at low stress and/or short times).
2. Reductions in properties induced by creep damage compounded by microstructural changes (e.g. cooled and/or shrouded first and second stage buckets operating at higher stress, or for very long times at lower stress).

The experimental program was conducted within the framework of a larger BWD Turbines project to develop improved analysis tools for gas turbine component failure analysis and life assessment.

The stress relaxation and constant displacement rate tensile tests in this investigation were performed by Materials Performance analysis, Inc. in Santa Barbara, California using test specifications and procedures developed by Dr. David Woodford. The details of the test procedure and the equipment required to conduct accelerated stress relaxation tests are described in detail by Woodford et al in 1992.

The nickel base superalloy, GTD111, developed by General Electric (GE) was selected for use in these experiments because of the general absence of published metallurgical and mechanical properties data pertinent to the alloy and its wide usage. The material is used extensively for high temperature rotating buckets in land-based gas turbines in both the poly-crystalline and directionally solidified forms in GE Frame 3, 5, 6,7 and 9 engine models.

The GTD111 material was characterized in four conditions (Table I). The material representing the standard heat treated condition was removed from the root form of bucket serial number EIFM203939. The metal temperature experienced in the root form during operation is relatively low ($< 540^{\circ}\text{C}$), thus the microstructural features and starting mechanical properties do not significantly change during service. This makes the root form material representative of the original chemistry and manufacturing process used to make the buckets and suitable material to base line the starting creep properties of the alloy.

Changes in creep strength due only to temperature based microstructural evolution (aging) were evaluated by testing sample material removed from the root form of bucket serial number EIFM204757 which was thermally exposed in a laboratory furnace at 900°C for 5000 hours.

The samples tested from the airfoils of the two service run buckets were from two different base loaded turbines operated on natural gas. The samples were tested to characterize the effects of combined microstructural evolution and accumulated creep damage. The airfoil sample removed from bucket EIFM203939 was from a cooler region of the lower airfoil where minimum service damage was expected to occur while the airfoil sample removed from bucket EIFM142492 was from the hottest region of the component where severe coating degradation and microstructural aging had occurred.

These particular service run buckets were selected as worst case examples to make sure that the test technique could discriminate between the various conditions and to set some lower bounds for future interpretation of the test data. The material tested was removed from old style, 11

hole bucket designs that were operated beyond predicted design temperatures. These buckets in no way represent the superior performance obtained in the latest GE MS6001 bucket designs that are in use today.

The microstructure, tensile properties and constant load creep rupture properties of the material used in these experiments were examined and reported on in detail by Daleo and Wilson (1996) and the failure mechanisms of aluminized MCrAlY coating systems applied to this generation of buckets were recently reviewed by Daleo and Boone (1997).

STRESS RELAXATION TESTING

The fundamental methodology and mathematics of stress relaxation testing was originally described by Soderberg (1936). Early examples of converting raw stress relaxation test data, stress versus time, to stress versus strain rate and using it to compare creep properties of austenitic stainless steels were published by Oding (1959). As better strain gaging and high speed digital data recording technology became available, methods of accelerating the test method using tensile testing machines were developed and used (Lee and Hart, 1971).

Today, using the Woodford test method and state of the art equipment, very accurate and reproducible tests can be performed. Five decades of creep rate can be covered in a test that takes approximately 20 hours to complete.

The use of stress relaxation test methods to help characterize creep properties of service run gas turbine components is a relatively new concept, first proposed by Woodford et al in 1992.

When Stress Relaxation Tests are performed under conditions of constant total strain, the total strain is defined by:

$$\epsilon_t = \epsilon_e + \epsilon_p \dots\dots\dots 1$$

Where ϵ_t =total strain, ϵ_e =elastic strain, and ϵ_p =plastic (creep) strain. The elastic strain is further defined by:

$$\epsilon_e = \sigma/E \dots\dots\dots 2$$

Where σ = stress and E = elastic modulus, therefore:

$$\epsilon_t = \sigma/E + \epsilon_p \dots\dots\dots 3$$

Under conditions where the total strain is held constant, plastic(creep)strain (ϵ_p) can only occur if the elastic strain (ϵ_e) decreases. Differentiating Equation (3) with time, remembering that the change in the total strain is zero,

$d\epsilon_t/dt=0$, results in the plastic(creep)strain rate ($d\epsilon_p/dt$), labeled $\dot{\epsilon}_p$, being defined as:

$$\dot{\epsilon}_p = -1/E \, d\sigma/dt \dots\dots\dots 4$$

The stress relaxation test data generated by the Woodford technique is in the form of stress to maintain the desired total strain versus time. A plot of stress versus the natural logarithm of time produces a straight line approximation of the relaxation decay curve. A least squares regression model $\sigma = \beta_0 + \beta_1 \ln t + e$ fitted to the curve describes the data in terms of stress versus in time. Differentiating the model with respect to $\ln(\text{time})$ and multiplying it by 1/t produces an expression for the stress rate, $d\sigma/dt$.

The stress rate is then inserted into the creep rate formula $\dot{\epsilon}_p = -1/E \, d\sigma/dt$ to calculate the creep rate. The data is best presented as a plot of stress versus the log of creep rate.

An expression of the stress rate, $d\sigma/dt$ can also be obtained using a power law fit of the raw data, $\sigma = \beta_0 + t^n + e$. A plot of stress vs time^N produces a straight line approximation of the relaxation decay curve. A least squares regression model ($Y = \beta_0 + \beta_1 X + e$) fitted to the data results in a fit of the data in terms of stress vs time^N . Differentiating the model results in the stress rate being defined in terms of $d\sigma/d(t^N)$ which can be converted back to stress rate ($d\sigma/dt$) by multiplying $d\sigma/d(\ln t)$ by $N * \text{time}^{(N-1)}$. (Values of N range from .01 to .001).

INVESTIGATION
1. MICROSTRUCTURAL ANALYSIS

Knowledge of the alloy microstructure is fundamental to understanding the mechanical property behavior of the material. Superalloy microstructures continually change with time at the operating temperatures experienced in most gas turbine applications.

The starting microstructure of the GTD111 buckets is a product of the chemistry, the casting parameters, coating and heat treatment steps used to manufacture the component. The buckets used in this study were vacuum investment cast, hot isostatically pressed, machined and processed through the GE GT29INPLUS coating process and the GE GTD111 alloy standard heat treatment.

The microstructural features generated by the processing were similar to other nickel based superalloy casting alloys previously described by Sims, et al, 1987. In general, all of the bucket castings examined appeared to be of high quality. No excessively large grains, porosity, or areas of gross shrinkage were observed.

The microstructures of the material used in this study were examined and reported on in detail by Daleo and Wilson (1996). A brief overview is presented here to help in the interpretation of the stress relaxation data.

The GTD111 microstructure in the standard heat treated condition consisted of a duplex gamma prime (γ') ($\text{Ni}_3(\text{Al},\text{Ti})$) precipitate evenly distributed in the face centered cubic (FCC) gamma (γ) matrix (Figure 1). The average size of the primary γ' precipitates was 0.86 micron and the average size of the secondary γ' precipitates was 0.1 micron. The grain boundaries were decorated with a very thin, discontinuous $\gamma'/\text{M}_{23}\text{C}_6/\text{M}_6\text{C}$ carbide layer (Figure 1). Scattered throughout the matrix and occasionally on the grain boundaries were eutectic γ' nodules and MC carbides ($\text{Ta},\text{Ti},\text{W}$). The grain boundaries were finely serrated and wavy on a macro scale. Eutectic γ' and MC carbides were present both along the grain boundaries and evenly distributed throughout the matrix.

The stability of the various microstructural phases at the operating temperatures experienced by gas turbine buckets is extremely important. In service the γ' phase increases in size with time and temperature, and complex carbide reactions occur. The most important of the carbide reactions is the continued growth of the M_{23}C_6 carbide phase along the grain boundaries. The migration of chromium to the boundary leaves the matrix locally enriched in the γ' forming elements nickel, aluminum, titanium etc. allowing a film of γ' to form along the boundary. Degeneration of MC carbides into $\text{M}_{23}\text{C}_6 + \gamma'$ in the matrix and along the grain boundaries accelerates the process. Examples of these phase changes were observed in the microstructure of the bucket thermally exposed at 900°C for 5,000 hours as well as in service exposed material.

The microstructure of bucket EIFM204757 after the 5,000 hour thermal exposure at 900°C is presented in Figure 2. The primary γ' precipitates had transformed from cubic shaped particles to a rounded morphology. The size of the primary γ' precipitates had grown from an average size of 0.86 micron to 1.16 micron. The secondary γ' precipitates were consumed. The grain boundary carbides had coarsened and coalesced. Thick continuous $\gamma'/\text{M}_{23}\text{C}_6$ films had formed.

The microstructure of a GTD111 turbine bucket removed from service after 23,000 hours is presented in Figure 3. Note that the matrix γ' , the grain boundary carbides and the formation of γ' films along the boundaries have continued to coarsen. The formation of γ' along grain boundaries is normal and in most cases beneficial. However, when the films become too thick, the boundary is embrittled,

becomes notch sensitive, and is prone to cracking. Continued growth of the γ' phase reduces the creep resistance of the material.

2. STRESS RELAXATION TESTS

Stress relaxation tests were performed on each sample at four different combinations of temperature and total pre-strain (850°C and 900°C at 0.4% and 0.8% pre-strain). A typical example of the test data, in the form stress versus log time, is illustrated in Figure 4. Plots of the data expressed in terms of stress versus log creep rate are illustrated in Figures 6 to 9.

2.1 Root Form, Standard Heat Treated Condition

The stress relaxation tests performed on the material in the standard heat treated condition were repeated on a second test bar two months after the first tests were made to determine the repeatability of the strain rate measurements and, to provide an estimate of the variance. The test results at all test conditions were duplicated with extremely good precision. An example of the reproducibility of the test results is presented in Figure 5.

2.2 Root Form, Furnace Exposed Condition

The stress relaxation tests done at 850°C at both 0.4% and 0.8% total strain conditions revealed that, compared to the material properties in the standard heat treated condition, the creep rate properties of GTD111 alloy were degraded by the 5,000 hour thermal exposure at 900°C. In the test run done at 0.8% total strain, the strain rate curve at the lower stress levels fell back onto the new material curve (Figure 7). This type of behavior is also observed in standard constant load creep rupture tests.

The stress relaxation tests done at 900°C at both 0.4% and 0.8% total strain did not detect the drop in properties in the thermally exposed material.

2.3 Service Run Airfoils

The stress relaxation tests completed at 850°C, indicated at both the 0.4% and 0.8% total pre-strain conditions, that the material properties, expressed in terms of creep rate for a given stress, had increased by up to two orders of magnitude. The stress relaxation tests done at 900°C at both the 0.4% and 0.8% total strain also indicated an increase in creep rate, unlike the thermally age material. However, the magnitude of the drop in properties measured at 900°C was not as large as in the tests performed at 850°C.

3. CONSTANT DISPLACEMENT RATE TENSILE TESTS

Constant Displacement Rate tensile tests were performed after the stress relaxation test runs to provide a quantitative measure of the materials strain tolerance in

each condition. The tests were performed at 800°C at a constant strain rate of 1% strain per hour. A plot of Stress versus Strain illustrating the test data is presented in Figure 10.

The yield points of the tensile curves were approximately 30% lower than what would be typically measured in standard tensile tests of GTD111 alloy. This is normal and is a result of the creep component associated with the test.

The strain tolerance of the material thermally exposed for 5000 hours at 900°C was dramatically reduced compared to the material in the standard heat treated condition, however the ultimate strength of the material had not deteriorated.

The service run buckets still possessed some creep ductility after operation. However the ductility compared to the material in the standard heat treated condition was significantly reduced. The ultimate strength of the service run material removed from the hottest section of bucket EIFM142492 had deteriorated, while the ultimate strength of the material from the cooler section of bucket EIFM203939 had not deteriorated.

DISCUSSION

1. APPLICATION OF STRESS RELAXATION TESTING IN METALLURGICAL LIFE ASSESSMENT

When the stress relaxation data is expressed in terms of stress versus creep rate, the material creep properties in different conditions can be compared directly in terms of temperature capability of the new material in the fully heat treated condition (Figure 11). In this plot, the stress relaxation tests performed at 850°C and 0.8% total pre-strain conditions indicated that the material properties of the service run airfoil material had decreased by the equivalent of almost 40°C. Note that the GTD111 material properties in the standard heat treated condition are presented as the mean regression line of the two data sets together with the 95% confidence intervals for individual readings and that the data sets were extrapolated to lower strain rates by two orders of magnitude.

To use this approach in life assessment applications, an estimate of the starting material properties generated by the original processing would be obtained by measuring the material properties in the root form at three temperatures that bracket the service temperature range of interest. The service run airfoil samples would then be measured at the two most relevant temperatures of interest. Plotting the data all together on one plot provides a direct estimate of the drop in creep rate properties in terms of temperature. Once the drop in temperature

capability is known, the extrapolation procedure of choice can be used to analyze the data. The creep rates of different materials tested in this manner can also be compared directly. This provides the material's engineer with a very powerful tool for new alloy development and for alloy selection in critical applications.

The differences observed between the fully heat treated GTD111 alloy and the degraded materials were found to be sensitive to the testing parameters (stress, temperature and pre-strain). In the test run done at 850°C and 0.8% total pre-strain, the stress versus strain rate curve for the microstructurally aged condition fell below the new material curve by almost an order of magnitude at the highest stress levels (Figure 7). However, the two curves ultimately converged at the lower stress levels, which are more typical of those actually encountered by rotating turbine buckets. As noted earlier, this type of behavior is also observed in standard constant load creep rupture tests. However, creep rupture tests conducted at the lower stress levels would require thousands of hours to reach completion, which is clearly impractical for the purposes of conducting a life analysis.

If the same result had been obtained on airfoil material taken from a service-exposed component, it might be concluded that the higher creep rates (corresponding to reduced stress rupture lives) determined at higher stresses were simply indicative of the normal change in the microstructure of the material which is brought about by service exposure. However, the similarity in creep rates at the lower stress levels would be an indication that the material has not experienced a significant degree of (unexpected) creep damage which could otherwise make it incapable of reaching its intended design life.

In contrast, the sample removed from the hottest area of bucket serial number EIFM142492 showed even greater reductions in creep strength as compared to the "new" material. At 850°C and 0.8% total pre-strain, the creep rates of the service-degraded airfoil material remained almost an order of magnitude higher than those of the new and furnace exposed samples, even at the lowest stress levels. In addition, the curve for the airfoil material did not show any indication of convergence with the two other samples. Based on the history of creep failures in this bucket design, it seems reasonable to conclude that these differences in measured properties can be attributed to the combined effects of microstructural aging and creep damage.

The differences in creep behavior at 900°C were not as pronounced as those observed at 850°C (Figure 9). This is probably an indication of the influence of the test parameters on the alloy microstructure and the

predominant creep mechanism that is controlling the creep rate of the material in the standard heat treated condition. The rate of dissolution of the secondary gamma prime particles are significantly higher at 900°C, and subtle changes occur in the grain boundary precipitate morphology. It has also been suggested that there may be a significant change in the activation energy for creep at temperatures close to those used in this investigation (Koul and Castillo, 1993). It is beyond the scope of this paper to discuss these effects in greater detail. We merely point out that, by specifying the appropriate test parameters, the stress relaxation test is a powerful tool, capable of distinguishing between different forms of material degradation that could be encountered by highly stressed gas turbine components.

Based on the observed differences in creep behavior, the stress relaxation test technique appears to be capable of distinguishing between the two limiting forms of material damage selected for this investigation. This is a very important and useful result since it indicates that the test could help to sort out the changes in creep strength as a result of (normal) microstructural evolution from the combined effects of microstructural evolution and strain related creep damage. This has historically been one of the uncertainties arising from the use of conventional creep rupture tests which are routinely performed as part of an overall metallurgical life assessment.

2.0 ESTIMATES OF RUPTURE LIFE BASED ON STRESS RELAXATION DATA

The mechanism resulting in fracture in the shortest time or after the lowest strain determines the failure characteristics of the material. In terms of creep mechanisms, time to failure is a function or a measure of the material's creep strength (ie. creep rate) while strain tolerance at failure is primarily a function of the microstructure.

Creep strength can be best thought of in terms of changes in the steady state or average creep rate ($\dot{\epsilon}$) with respect to time, stress and temperature.

$\dot{\epsilon} = f(t, \sigma, T) \dots \dots \dots 5$

The most widely accepted (used) expression for $\dot{\epsilon}$ is:

$\dot{\epsilon} = B \sigma^n e^{(-Q_c/RT)} \dots \dots \dots 6,$

where B and n are constants, σ =stress, Q_c is the activation energy for creep (KJ/mole), R is the universal gas constant (8.314 KJ/mole) and T= temperature in °K.

Recognising that the time for rupture, t_r , is also a function

of the creep rate (Monkman Grant ($t_r \propto 1/\dot{\epsilon}$) and many more sophisticated models to follow), the rupture life can then be expressed as:

$1/t_r \propto \dot{\epsilon} = B \sigma^n e^{(-Q_c/RT)} \dots \dots \dots 7$

The stress relaxation test can be thought of as taking a cross section through a series of constant load creep rupture curves at a set total strain and temperature. At 0.8% total strain, in most constant load creep rupture curves, the steady state creep rate has been reached. Thus in a single stress relaxation test an estimate of the steady state creep rate is obtained over a large range of stress conditions.

The time to failure at any given stress and temperature combination can therefore be estimated directly from the creep rates measured in the stress relaxation test runs.

The Monkman-Grant method of relating rupture lives to minimum creep rates is not really applicable here, since it is based on a simple correlation between minimum creep rates and rupture lives, as measured in constant load creep rupture tests. However, at the optimum total strain parameter of each alloy, the stress relaxation test provides a measure of the average steady state creep rate. This allows a more precise estimate of creep rupture life to be extracted from the data by dividing the expected or the minimum acceptable fracture elongation directly by the measured creep rate.

The poly-crystalline GTD111 superalloy system examined in this study exhibit creep ductilities that range from a low of about 5% to approximately 15% when measured in standard constant load creep rupture tests. Thus a plot of stress vs calculated life based on 5%, 10%, and 15% elongation at any particular temperature would provide not only a measure of the expected life but also an indication of the possible scatter to be expected (Figure 12). In fact a universal plot of life vs strain rate can be produced and used (Figure 13).

One could argue that the accuracy of the estimate of the time to rupture will be slightly non-conservative because no account has been made for the creep rates during primary and tertiary creep. However because the creep rate measured by the stress relaxation technique is an average instantaneous value, the errors are minimized.

The data sets examined in this study indicate that rupture lives can be estimated to within a factor of three, which is quite remarkable since the data needed to estimate rupture properties can be generated and analyzed within a few weeks.

3.0 CORRELATION OF STRESS RELAXATION TEST DATA WITH TIME-TEMPERATURE PARAMETER APPROACHES

A Larson-Miller curve was produced by converting the rupture time estimates generated by this method into Larson-Miller format (Larson and Miller, 1952) and fitting the data into a best fit curve using a least squares regression model ($Y = \beta_0 + \beta_1 X + e$). Comparing the plot made using the estimated data with published Larson-Miller plots in the open literature (Schilke, 1992; Daleo, 1996) indicates that this technique can rapidly produce these plots with reasonably good accuracy, Figure 14. This technique was also used to produce Larson Miller plots for two other widely used gas turbine blading alloys, IN-738LC and IN-939, Figures 15 and 16, for which stress relaxation data had been previously obtained (Woodford, Daleo & Wilson).

Note that the plotted points in Figure 14 below about 175 MPa, or strain rates below about $1 \times 10^{-4} \text{ h}^{-1}$ are based on extrapolations of the linear fits to the experimental data shown in Figures 7 and 9.

The creep rates measured at the various temperatures for any given total strain can be directly parameterized using common prediction algorithms such as the Larson Miller Parameter, $P = T(C - \log_{10} \dot{\epsilon})$ described by Conway (1965) and illustrated in Figure 17.

Alternatively, the creep rate plots can be parameterized using Equation 6 ($\dot{\epsilon} = B \sigma^n e^{-(Q_c/RT)}$). By converting the equation into logarithmic form, an estimate of the activation energy for creep can be obtained by systematically varying the activation energy for creep until a plot of $\ln \dot{\epsilon} + Q_c/RT$ versus $\ln \sigma$ aligns the creep rate curves at the various test temperatures into one line. The slope of this line provides an estimate of n directly while the intercept provides an estimate of B in the form of $\ln B$.

$$\ln \dot{\epsilon} = \ln B + n \ln \sigma - Q_c/RT \dots \dots \dots 8$$

The data from the sample in the standard heat treated condition tested at 850°C and 900°C at 0.08% total strain was parameterized in this form and is presented in Figure 18. The activation energy for creep was estimated at 725 KJ/mole and from the plot, the constants B and N were estimated at 3.9512 and 10.2 respectively. Inserting the estimation of the activation energy and the constants back into equation 6, the creep rates were then calculated and compared to the measured creep rates from the stress relaxation tests Figure 19. A reasonable approximation of the original test data was obtained indicating that with a little more effort a better creep model could be established to use the creep relaxation data.

SUMMARY AND CONCLUSION

When combined with our comprehensive metallurgical evaluation methods for gas turbine failure analysis and life assessment, the stress relaxation test methodology can be a very powerful tool in helping to quantify degradation of creep properties in service run components. The speed at which the testing and analysis can be performed now makes realistic life assessment and repair replace decisions possible during turbine overhauls.

The unique ability to measure changes in creep rate over a large stress range, enabled the technique to distinguish changes in creep strength due to (normal) microstructural evolution from the combined effects of microstructural evolution and strain related creep damage.

The creep rate data measured in the stress relaxation tests can be used in its direct form, where the creep rates of the material in different conditions are compared directly in terms of temperature capability or by estimating the time to failure at any given stress and temperature combination. The data sets examined in this study indicate that rupture lives can be estimated within a factor of 3.

The stress relaxation tests performed on the GTD111 material removed from the old style 11 hole bucket designs revealed that, compared to the material properties in the standard heat treated condition, the creep rate properties in the bucket airfoil were deteriorating in service. The stress relaxation tests done at 850°C at 0.8% total strain indicated that the material properties had decreased by an order of magnitude or approximately 40°C.

The direct measurement of the creep strength using the stress relaxation test method described in this paper provides the component designer with a very efficient way of comparing creep strengths of different materials and also accurately predicting failure times. The analysis techniques can be used to examine a wide range of components (blades, vanes, discs etc.) from all makes of turbines, as well as in numerous other areas of endeavor where creep problems exist. For example, the test methodology can be used to assess the quality and the amount of material rejuvenation that actually occurs during component repairs involving regenerative HIP and re-heat treatment cycles or to examine the strength of welded or brazed, joints and thermal spray powder build ups.

ACKNOWLEDGMENTS This work was partially funded by the National Research Council of Canada's Industrial Research Assistance Program.

REFERENCES:

1. Conway J.B. "Stress-Rupture Parameters: Origin, Calculation and Use", 1965, Gordon and Breach, Science Publishers.
2. Daleo J.A. and Boone D.H., "Metallurgical Evaluation Techniques In Gas Turbine Failure Analysis And Life Assessment", Failures 96, Risk, Economy and Safety, Failure Minimization and Analysis, 1996 Balkema, Rotterdam. ISBN 90 5410 8231, Edited by R.K Penny.
3. Daleo J.A., Wilson J.R., "GTD111 Alloy Material Study", ASME Paper 96-GT-520.
4. Daleo J.A. and Boone D.H., "Failure Mechanisms of Coating Systems Applied to Advanced Turbine Components", ASME Paper 97-GT-486.
5. Koul A.K, Castillo R., "Creep Behavior of Industrial Turbine Blade Materials", Advanced Materials and Coatings for Combustion Turbines" ASM International, 1993, ISBN 0-87170-487-0.
6. Larson F.R., Miller J., Trans. ASME 74, 765 (1952).
7. Lee D., Hart E.W., "Stress Relaxation and Mechanical Behavior of Metals" Metallurgical Transactions 1971, Vol 2, pages 1245-1248.
8. Monkman F. C., Grant N.J., "An Empirical Relationship Between Rupture Life and Minimum Creep Rate in Creep Rupture Tests", Proc. ASTM, Vol 56, pg 593, 1956.
9. Oding I. A. et al., "Creep and Stress Relaxation in Metals", 1959, Academy of Sciences of the U.S.S.R., English translation by A.J.Kennedy, Oliver and Boyd Limited.
10. Schilke P.W., Foster A.D., Pepe J.J., and Beltran A.M., "Advance Materials Propel Progress in Land-Base Gas Turbines", Advanced Materials And Processes, April/1992.
11. Sims C.T.,Stoloff N.S., Hagel W.C. editors, Superalloys II, A Wiley-Interscience Publication 1987.
12. Soderberg C. R., "The Interpretation of Creep Tests for Machine Design," Trans. ASME vol. 58, p733, 1936.
13. Woodford D.R., Van Steele K., Amberg K., Stiles D., "Creep Strength Evaluation for IN 738 Based on Stress Relaxation", Superalloys 1992, edited by Antolovich S.D. et al, The Minerals, Metals and Materials Society.
14. Woodford D.R., Daleo J. A., Wilson J. R., "Analysis of Service Run Ruston TB5000 Components", 96Mpa / W&D

01, 1996, Materials Performance analysis/Wilson & Daleo Inc. internal report.

Table I

Serial Number	Heat Code	Sample Location	Condition
EIFM203939	VAF140	Root Form	Standard Heat Treatment
EIFM204757	VAF141	Root Form	Standard Heat Treatment + 5000 hours @ 900°C
EIFM142492	VAF108	60% Airfoil Height, Suction Side Between Holes 3 & 4.	23,000 Hours of Service
EIFM203939	VAF140	10% Airfoil Height, Pressure Side Between Holes 3 & 4.	19,150 Hours of Service

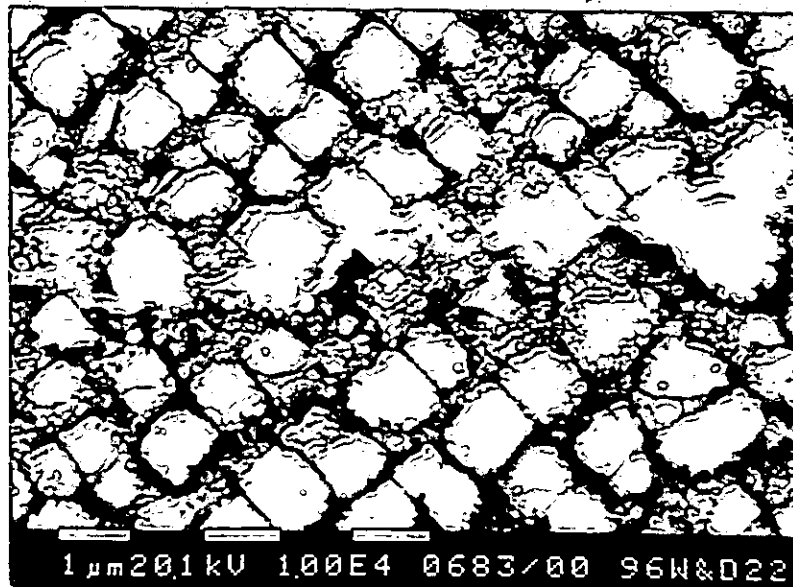
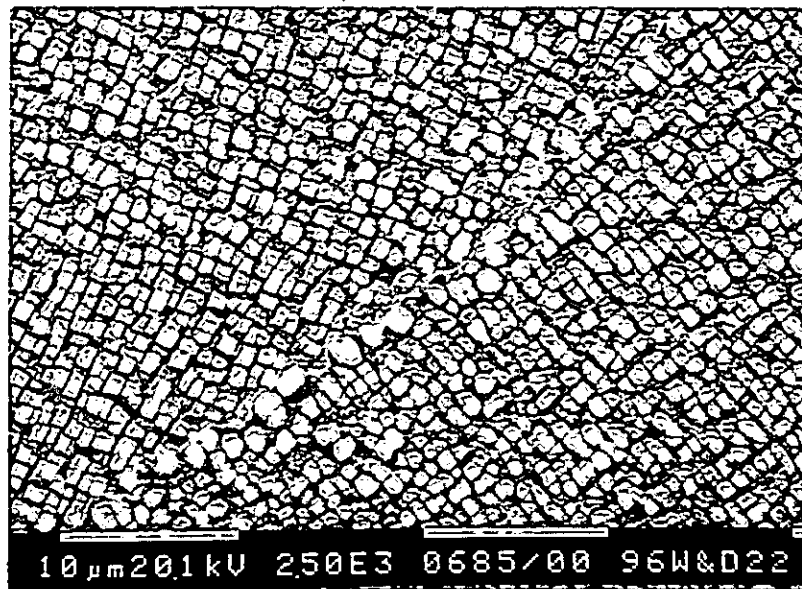


Figure 1. Scanning Electron Micrographs of the GTD111 microstructure in the standard heat treated condition illustrating the duplex gamma prime precipitate structure and the grain boundary carbide morphology.

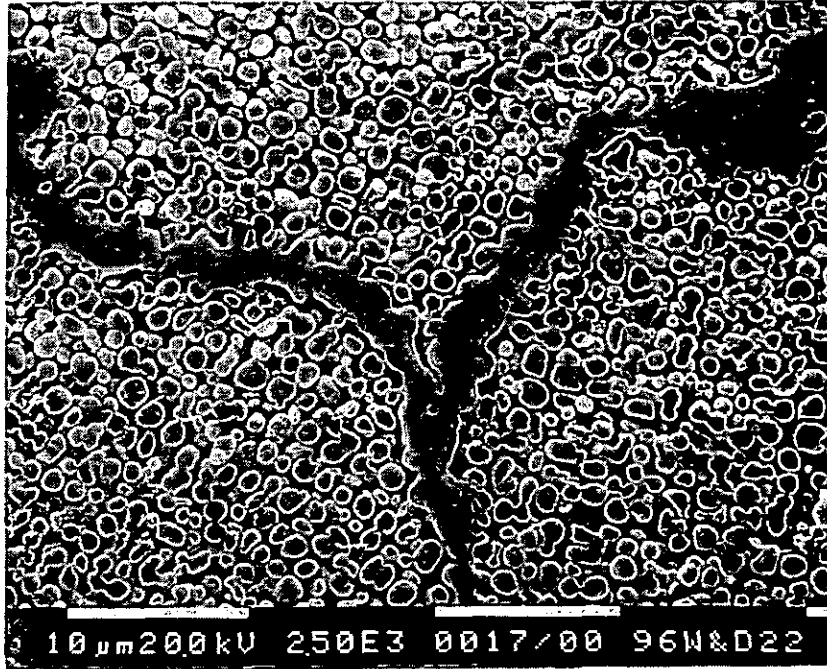


Figure 2. A Scanning Electron Micrograph illustrating the GTD111 microstructure after a 5,000 hour thermal exposure at 900°C (1650°F).

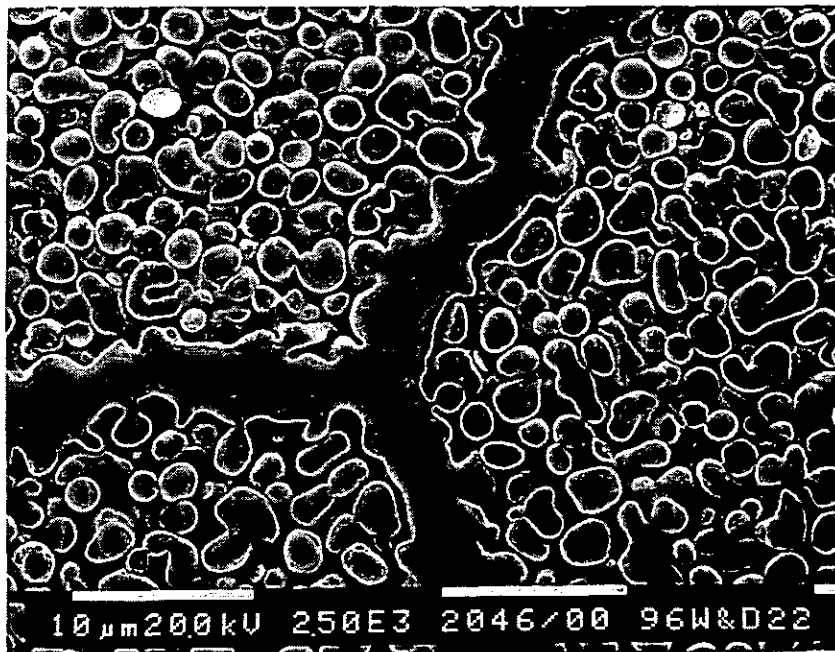


Figure 3. A Scanning Electron Micrograph illustrating the GTD111 microstructure observed at the 50% airfoil height location of the leading edge after 23,000 hours of service.

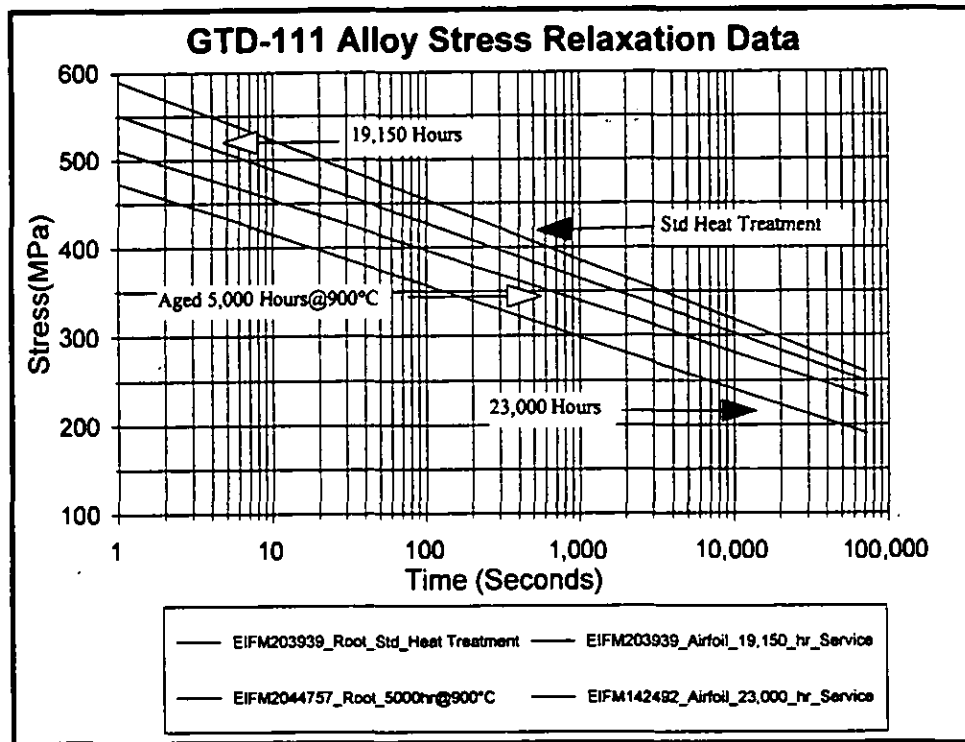


Figure 4. A plot illustrating the GTD111 alloy stress relaxation test data at 850°C and 0.8% total strain.

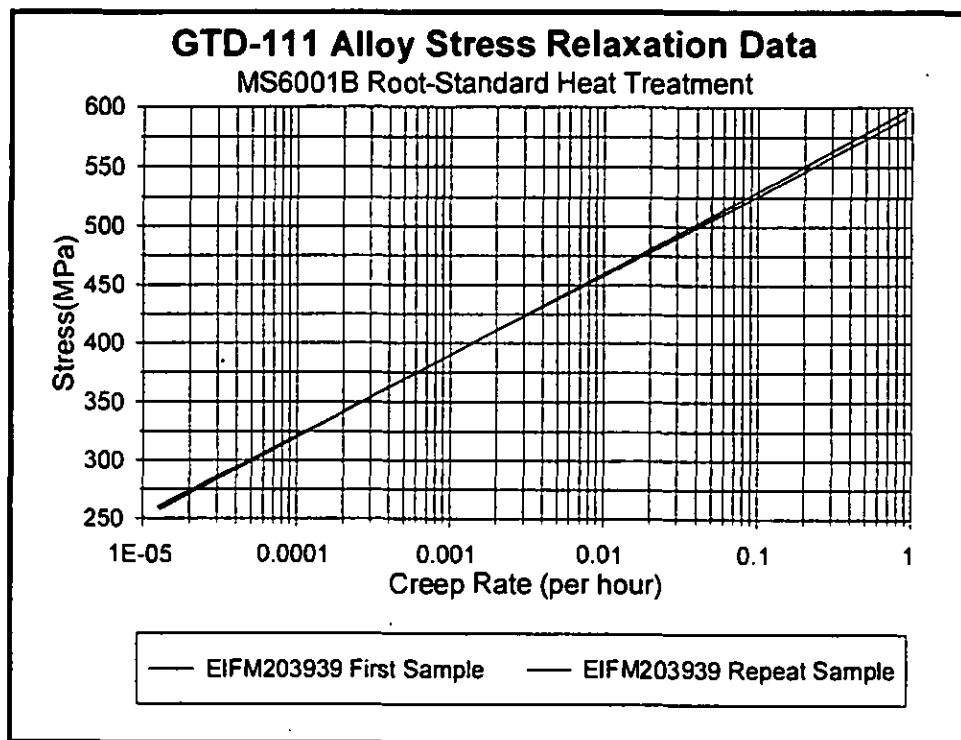


Figure 5. A plot illustrating the repeatability of the strain rate measurements measured on a second test bar tested two months after the first test. Test parameters, 850°C and 0.8% total strain.

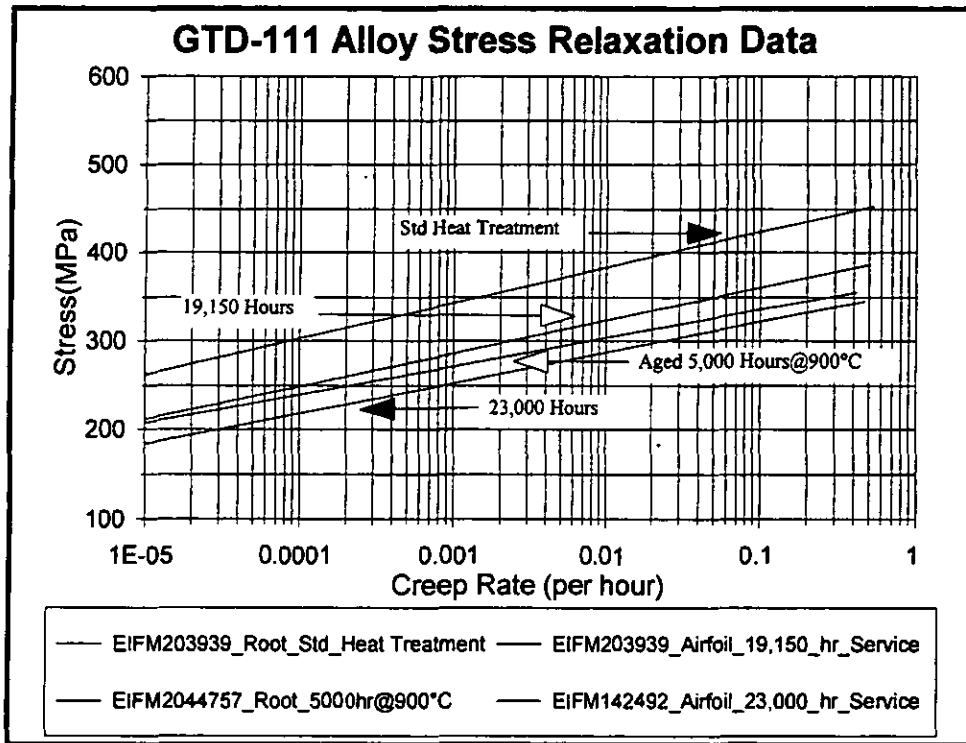


Figure 6. A plot illustrating the strain rate data measured from the samples at 850°C and 0.4% total strain.

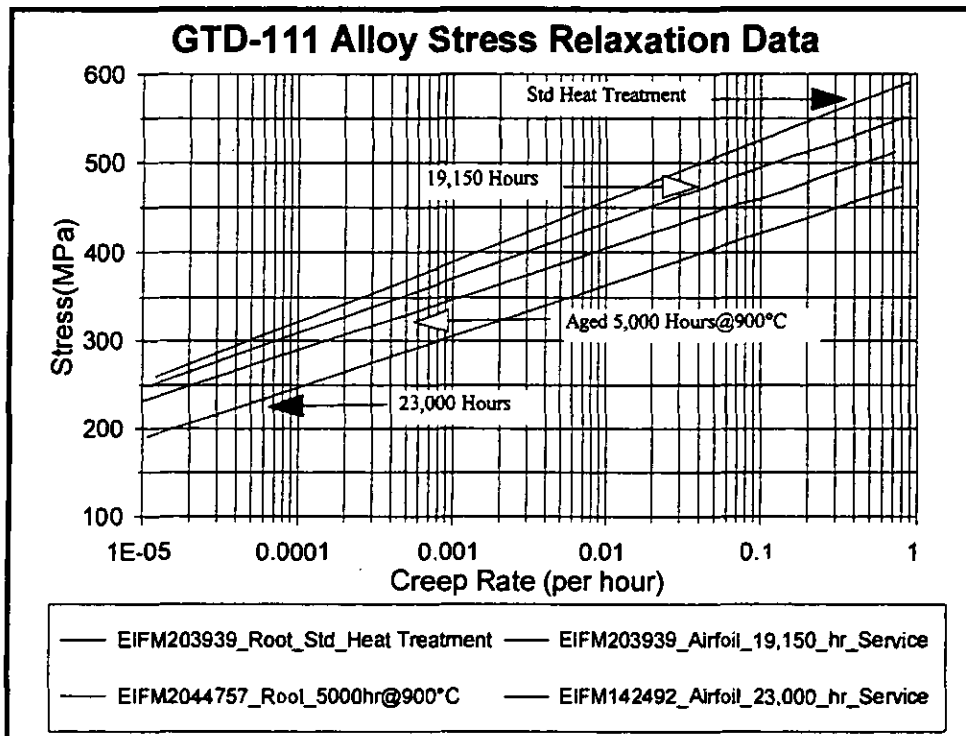


Figure 7. A plot illustrating the strain rate data measured from the samples at 850°C and 0.8% total strain.

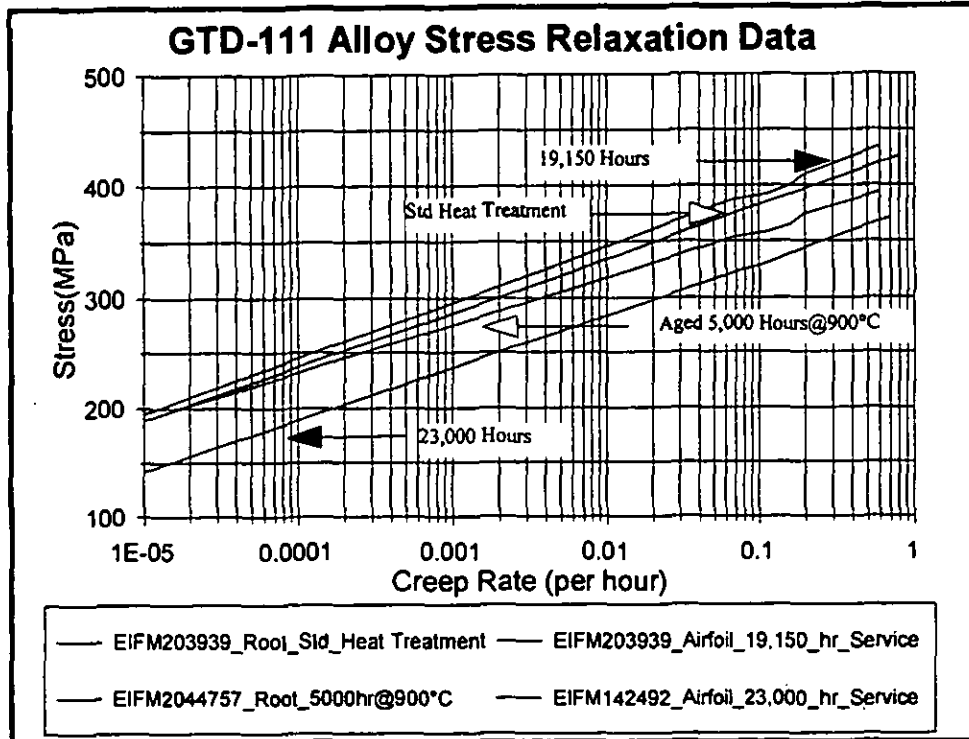


Figure 8. A plot illustrating the strain rate data measured from the samples at 900°C and 0.4% total strain.

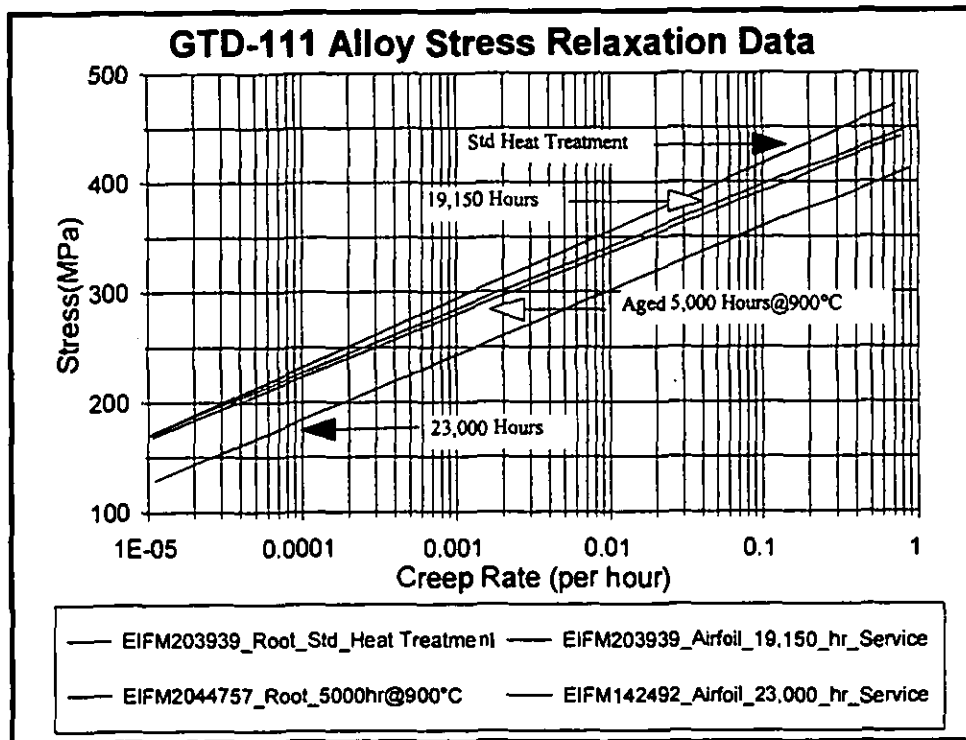


Figure 9. A plot illustrating the strain rate data measured from the samples at 900°C and 0.8% total strain.

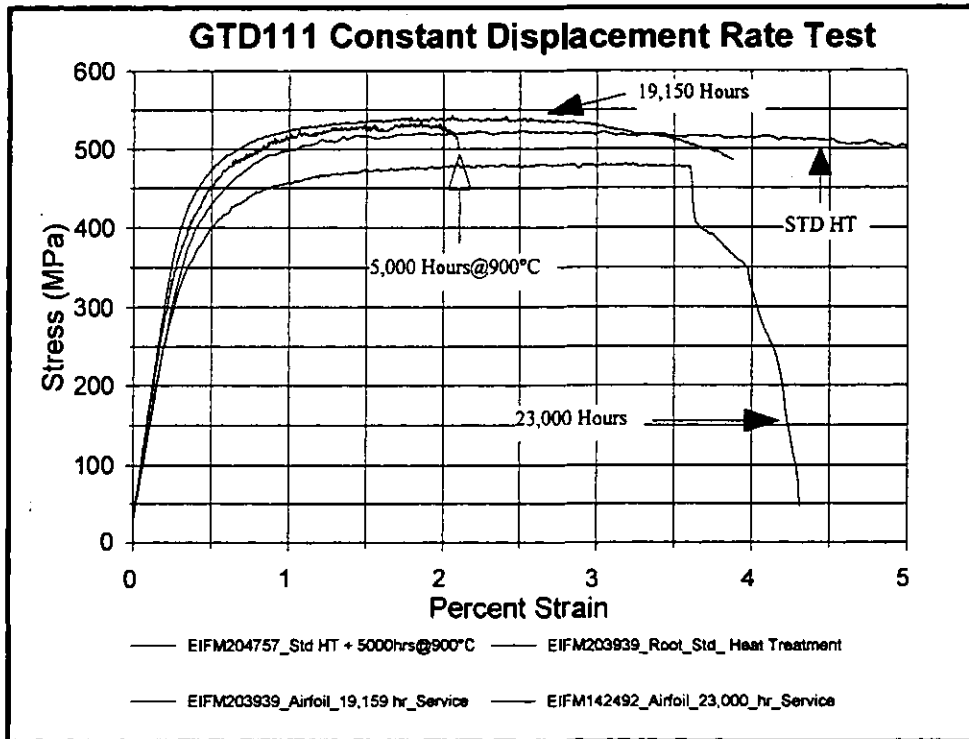


Figure 10. A plot illustrating the Constant Displacement Rate tensile data measured from the GTD111 alloy samples at 800°C and 1% strain per hour.

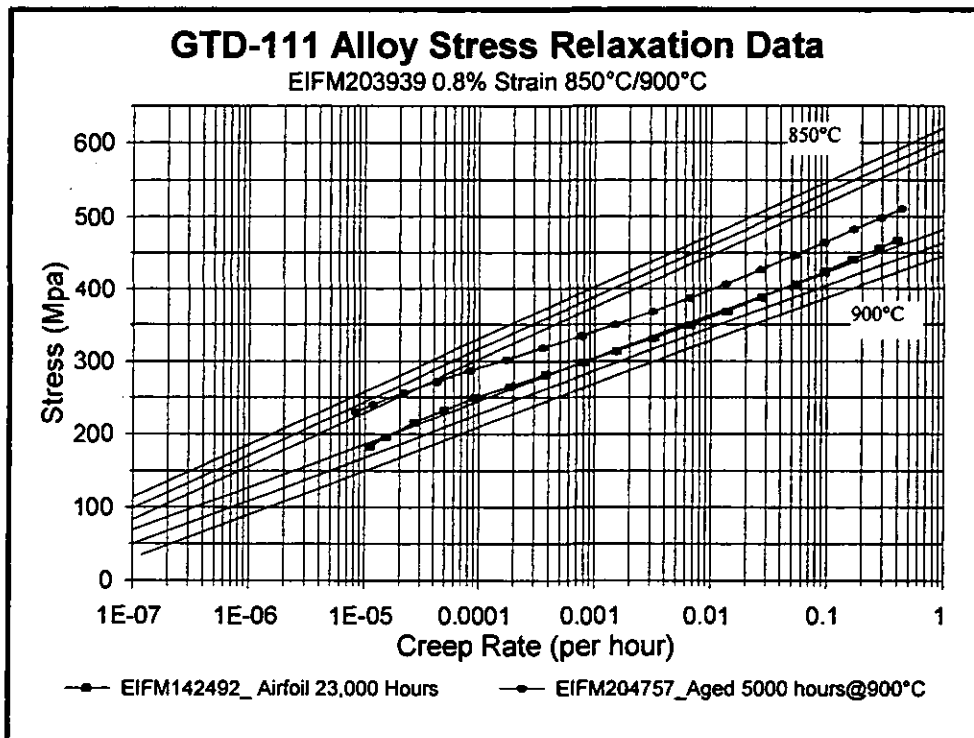


Figure 11. A plot illustrating the drop in creep rate properties measured in the bucket airfoil in terms of temperature capability of 'new' material in the standard heat treated condition.

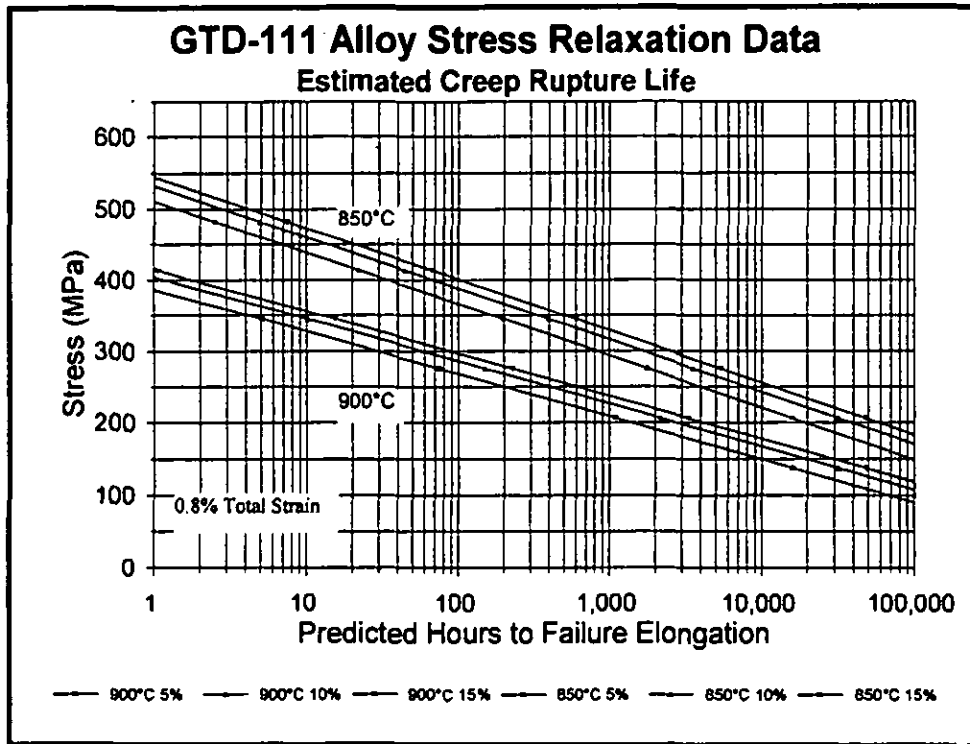


Figure 12. A plot of stress versus estimated creep rupture life of the root form material in the standard heat treated condition based on 5%, 10%, and 15% failure elongations.

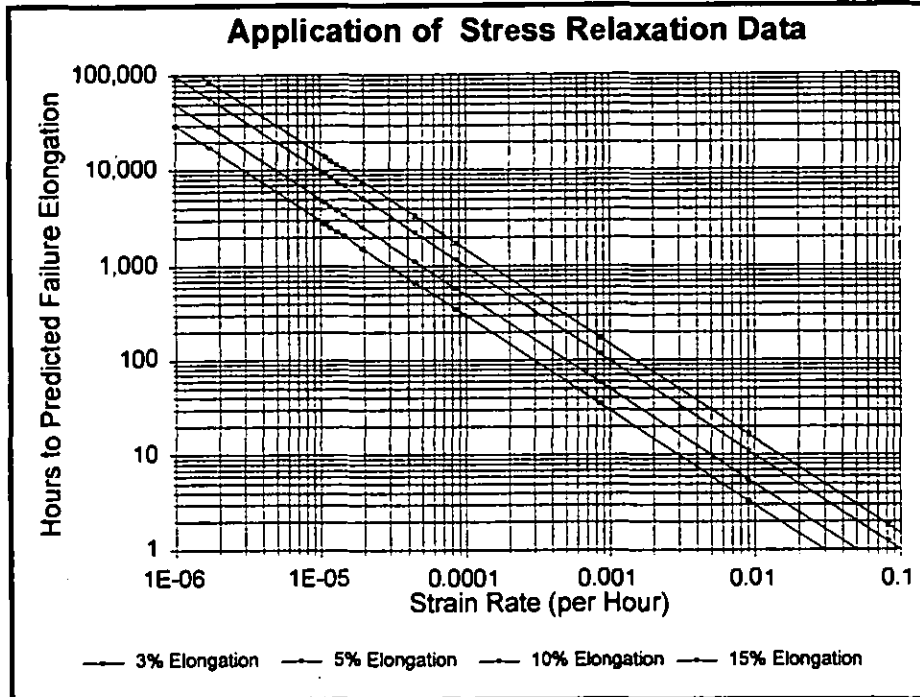


Figure 13. A master plot of stress versus estimated creep rupture life based on 3%, 5%, 10%, and 15% failure elongations.

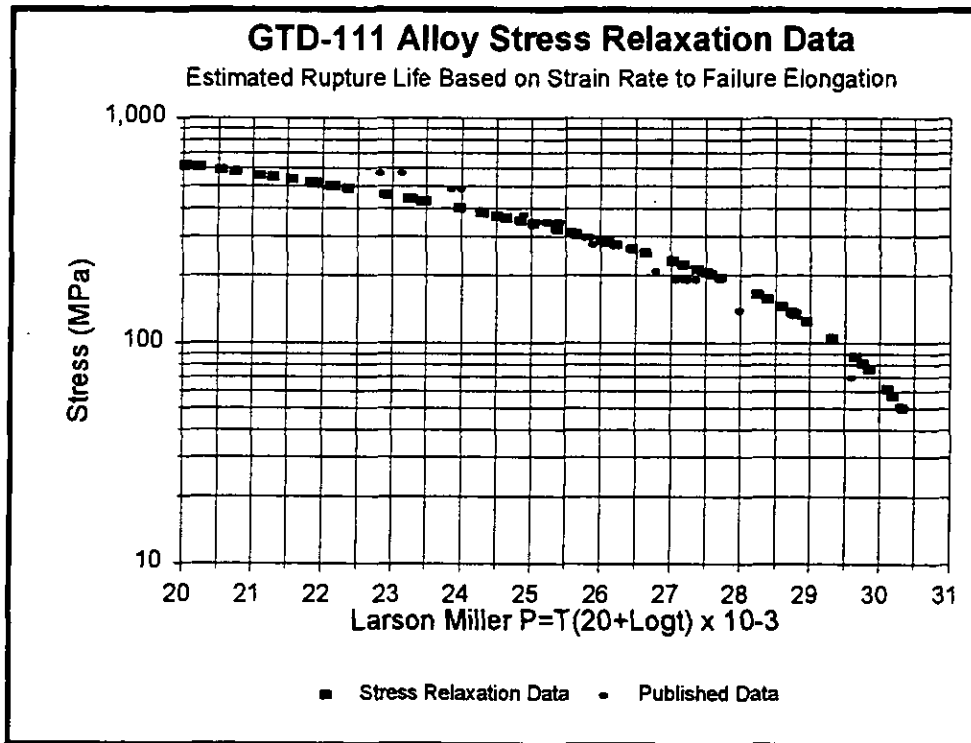


Figure 14. A plot comparing a Larson-Miller curve created from estimated creep rupture life based on strain rate to failure elongation, to published GTD111 creep rupture data.

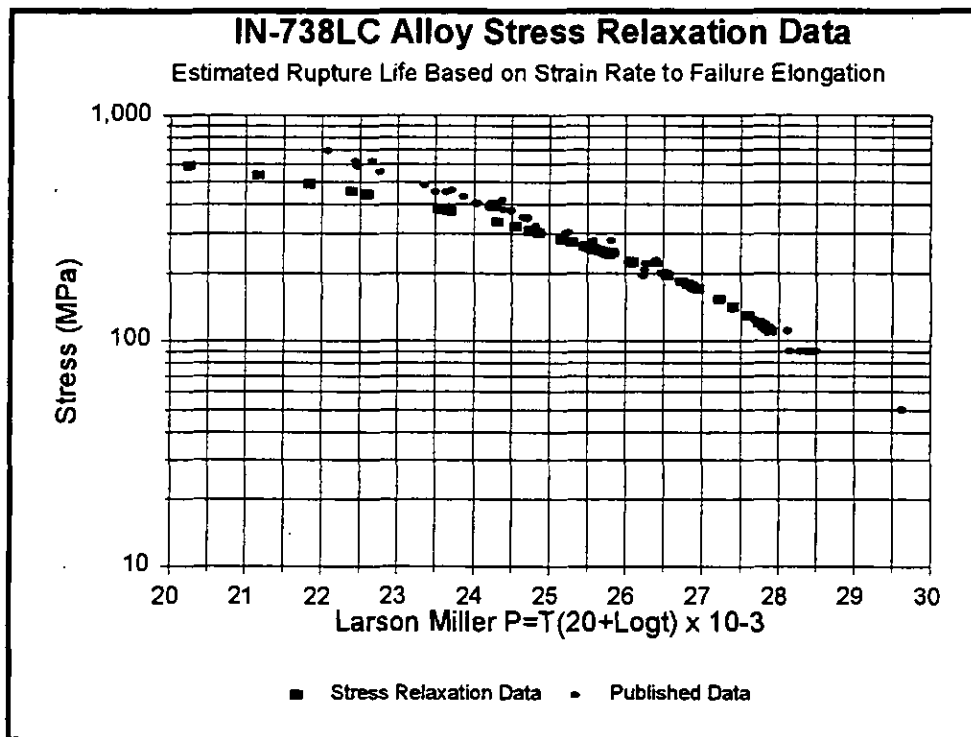


Figure 15. A plot comparing an IN-738LC Larson-Miller curve created from estimated creep rupture life based on strain rate to failure elongation, to published IN-738LC creep rupture data.

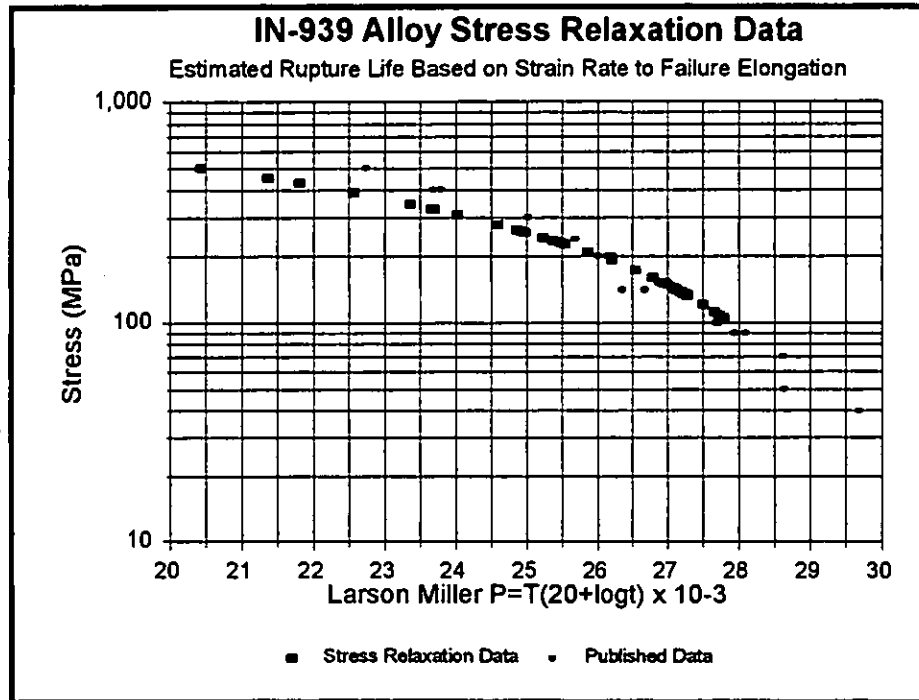


Figure 16. A plot comparing an IN-939 Larson-Miller curve created from estimated creep rupture life based on strain rate to failure elongation, to published IN-939 creep rupture data.

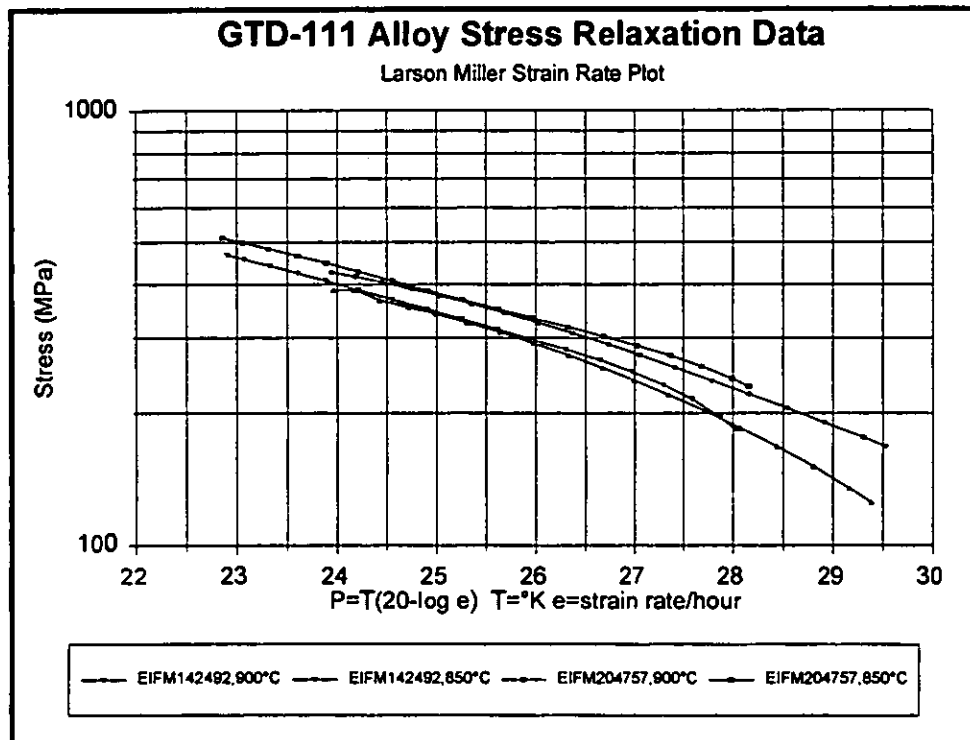


Figure 17. A Larson Miller strain rate plot illustrating the GTD111 strain rate data for the service run condition and the test sample exposed for 5,000 hours at 900°C.

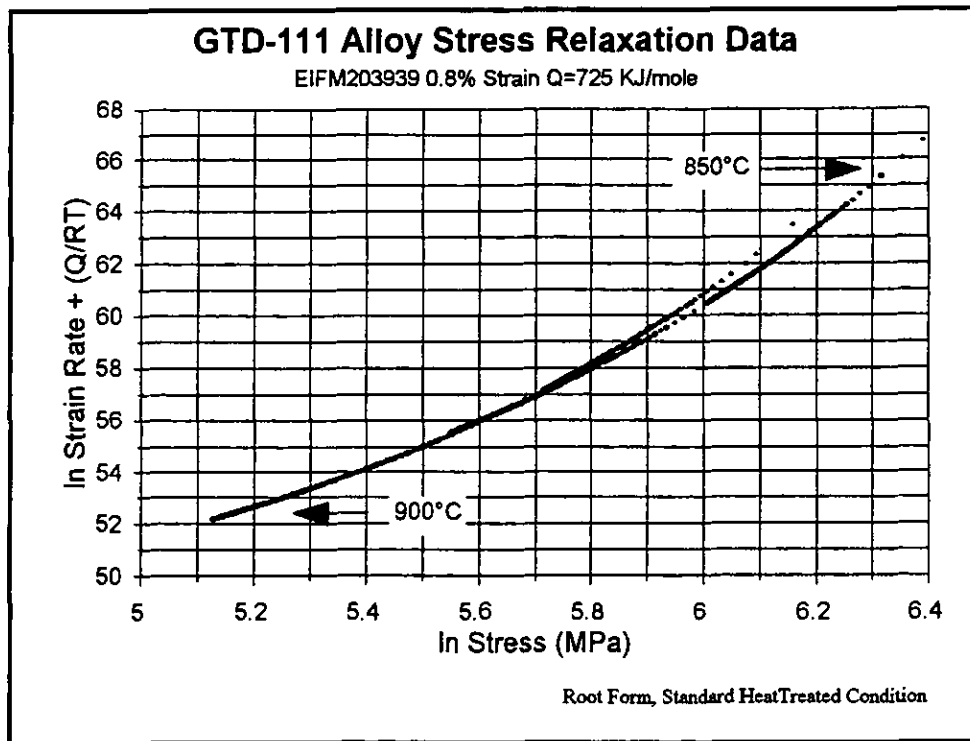


Figure 18. A plot illustrating the GTD111 strain rate data at 850°C and 900°C for the standard heat treated condition with the temperature dependence of creep rate represented in terms of the activation energy for creep.

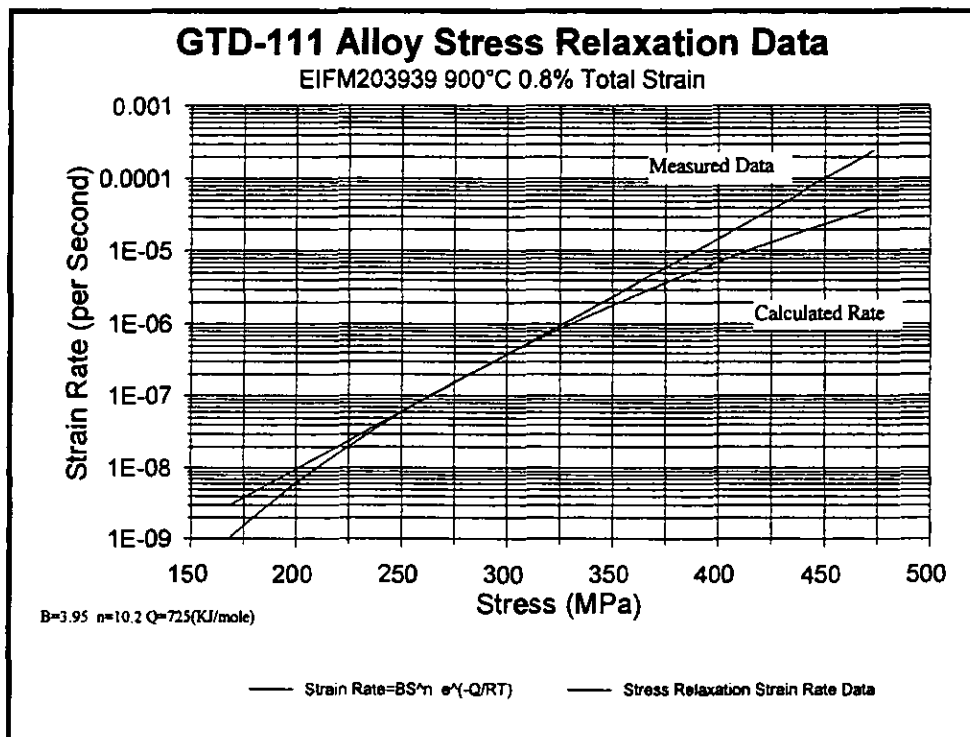


Figure 19. A plot illustrating the calculated strain rate ($\dot{\epsilon} = B \sigma^n e^{(-Q_c/RT)}$) versus the strain rate measured in the stress relaxation test for the standard heat treated condition at 900°C / 0.8% strain.